Generation of terahertz radiation by a moving bunch of nonequilibrium electron-hole plasma

V. N. Truchin and A. V. Andrianov
A. F. Ioffe Physical Technical Institute, 194021 St. Petersburg, Russia

N. N. Zinov'ev*
Department of Physics, Durham University, Durham DH1 3LE, United Kingdom
and A. F. Ioffe Physical Technical Institute, 194021 St. Petersburg, Russia
(Received 9 July 2008; revised manuscript received 8 September 2008; published 29 October 2008)

We report on properties of coherent radiation from nonequilibrium electron-hole (*e-h*) plasma bunch excited by an ultrashort laser pulse crossing a semiconducting slab subject to transverse bias voltage. Self-consisted calculations of nonequilibrium Boltzmann and Maxwell equations have established the fundamental role of uniformly moving bunch of *e-h* plasma in coherent generation of terahertz radiation. We have shown that predicted properties crucially depend on the physics of dissipation mechanisms, current configurations, and relative traveling velocities of *e-h* plasma bunch and terahertz radiation pulse. It has distinguished two major regimes of terahertz emission, single pulse emission, and firing twinned pulses at the moments of creation and extinction of moving bunch of *e-h* plasma related to the front and rare boundaries of semiconducting slab, respectively. The results of developed theory are applied to enhance the performance of photoconductive terahertz emitters.

DOI: 10.1103/PhysRevB.78.155325 PACS number(s): 72.30.+q, 41.60.−m, 72.20.Jv

I. INTRODUCTION

Optics with single-cycle or few-cycle pulses of electromagnetic (EM) radiation (EMR) has attracted a considerable attention during the last two decades.[1–3] The use of such pulses, whose spectral bandwidth falls into terahertz (THz) band of EM spectrum, presents particular interest as potentially unique informative probe for spectroscopically resolved imaging and microscopy. This growing interest is motivated by the demands of wealth of practical applications in physical and life sciences related to more precise analytical technologies using terahertz radiation.

Although the research on terahertz emission from semiconductors has been carried out for quite a while, the problem of identifying the mechanisms of emission is sill far from being complete and understood. A number of mechanisms are currently proposed to treat the emission of external terahertz field. They can be grouped into three categories: nonlinear conversion of pump beams in nonlinear materials, the emission mechanisms associated with photoelectric effects due to the surface built-in electric field, and the Dember field in bare semiconducting plates and emission of terahertz radiation by transversely biased semiconducting chip. Generation of a broad band coherent terahertz EMR can be accomplished using nonlinear interactions of EM waves in a suitable nonlinear semiconducting or insulating crystalline medium, recently considered in details in Refs. 4 and 5. The first group of photoelectrical generation of terahertz radiation forms the basis of terahertz emitters using a bare semiconducting slab. The photoinjected electrons and holes are accelerated in opposite directions by the surface built-in electric field, causing the drift current, $\mathbf{J}(t)$, to flow. This is the so-called current surge effect driven by surface built-in electric field.[6] There is another mechanism that can produce terahertz generation from a bare semiconducting slab. Under surface photoexcitation, the diffusion-recombination processes provide photoinduced fluxes with a net charge (let it be the electron charge) that is canceled by the charge associated with the accompanying screening mode (let it be the hole charge). Such diffusion flux is called ambipolar diffusion. The ambipolar diffusion flux itself is a weak current and varies slowly with time. It, however, creates a dipole layer (the Dember polarization dipole) and accompanies front to back voltage difference (the Dember voltage). It is this complex Dember dipole, $\mathbf{P}_D$, that plays the role of the source in generation of electromagnetic radiation.[7] The value of transient photocurrent in this case is given by $\mathbf{J}(t)=\frac{\partial \mathbf{P}_D}{\partial t}$. A characteristic feature of the first type of terahertz emitters is the longitudinal current or dipole in relation to the direction of excitation beam. The application of a magnetic field $\mathbf{B}$ perpendicular to the direction of light propagation yields the Hall equivalent of photocarriers' diffusion called photoelectromagnetic (PEM) effect and treated theoretically by van Roosbroeck[8] and, later, by Dixon[9] and by Chau and Elezzabi.[10] Numerical simulations of these effects can be carried out using Monte Carlo methods.[11] The second group of photoelectrical terahertz emission mechanisms can be realized in a semiconducting chip with a patterned in-plane layout of two surface contacts fabricated on the top of semiconducting substrate and biased with the external voltage source. Such terahertz emitters are called photoconductive antennas (PCA). It is assumed that photoexcitation of the semiconducting gap in a PCA creates nonequilibrium *e-h* plasma causing a burst of transient current between the contacts, $\mathbf{J}(t)$.[12–15] This current is considered as a transverse current against the direction of excitation beam.

We shall restrict our consideration to the second type of terahertz photoelectric emitters, namely, to PCA, ignited by an excitation of semiconducting gap with an ultrashort few-cycle laser pulse. It is assumed that according to Maxwell equations the burst of photocurrent in the switch gap creates the external EM field within a wide band of frequencies determined by the width of photocurrent pulse. One of the first

devices of this type was demonstrated in Ref. 12. PCA chip was exposed to the illumination with ultrashort laser pulses creating nonequilibrium electron-hole (e-h) pairs in the PCA and consequently a burst of photocurrent. Because of such seeming simplicity of physics underlying PCA functions, as well as demonstration, in many cases the highest yield of terahertz radiation, PCA has been a subject of experimental studies in many papers.[13–22] Quite the opposite, theoretical treatments of this problem have received far less attention. In most of published works the analysis of PCA emission mechanisms was performed within the framework of approaches that could be divided into three categories. In Refs. 16 and 18 PCA has been modeled as a dielectric slab with a surface oscillating current within the duration of optic pulse. Within the framework of this model the EM field irradiated into free space from PCA is calculated using the boundary conditions (BC) for **E** and **H** fields including the surface current. The surface current is phenomenologically introduced in this model. Such an approach, as we shall see below, may not adequately conform to the experimental situation with a finite absorption length that is comparable with the optical length of ultrashort laser pulse. The authors of Refs. 19 and 21, using the ideas and findings of Refs. 14 and 15, considered PCA on the base of semiempirical model of a capacitive semiconducting inset excited into a spot of a small diameter adjacent to PCA anode. In the third group of papers, represented here by Ref. 22, a generic simplified Drude model was applied to treat surface photocurrent in PCA. We also mention numerical simulations of three-dimensional (3D)-carrier dynamics[23] and analytical calculations based on density-matrix formalism in the Airy representation.[24] Regardless the particular model of terahertz emitter in the references cited above the electric field of terahertz radiation in the far field, E_{THz}, is treated as the emission from a point surface built-in electric dipole or current element induced by optical pulse excitation. Therefore, the following expressions are used to calculate the field: $E_{\mathrm{THz}} \propto \frac{\partial \mathbf{J}(t)}{\partial t}$ or $E_{\mathrm{THz}} \propto \frac{\partial^2 \mathbf{P}(t)}{\partial t^2}$, where $\mathbf{P}(t)$ and $\mathbf{J}(t)$ are the dipole moment and transient current element, respectively.[25]

The models used in the treatments cited above do not take into account the effects of nonequilibrium e-h plasma expansion and traveling of optical pump pulse in depth of semiconducting slab, as well as proper consideration of the source current and spatial distribution of EMR generated at plasma motion. The necessity and importance of taking into account plasma motion follows even from the simple comparison of characteristic times. Thus, the time required for an ultrashort optical pulse of the duration $\tau_0 = 10-100$ fs to cross a semiconductor slab of the thickness $d \sim 100-400$ μm is of the order of $t_b \sim 1-5$ ps. Such typical hierarchy of times, $\tau_0 \ll t_b$, requires theoretical consideration of a nonstationary regime of e-h plasma generation, including the effects of plasma expansion, configuration of currents in plasma, light-induced transfer effects due to coupling of traveling excitation pulse, and generated e-h plasma that could develop themselves in markedly different ways at the conditions of $\alpha d < 1$ and $\alpha d > 1$, where α is the absorption coefficient of the pump pulse. So far many important details of nonequilibrium e-h plasma dynamics on short time scale and interaction of plasma currents with electromagnetic field have not been properly attended including wavelength-time properties of EMR generation in plasma. In this paper we consider the theory of terahertz EM pulse generation by a moving bunch of nonequilibrium e-h plasma considering self-consistently photocurrent calculated from the first principles employing nonequilibrium Boltzmann equation and the generation of external EM field by the photocurrent source under the conditions of propagating pump laser pulse inside a semiconducting slab. Numerical calculations and graphic presentations demonstrate the application of this theory to the practical examples of PCA with semiconducting slabs of GaAs and Si.

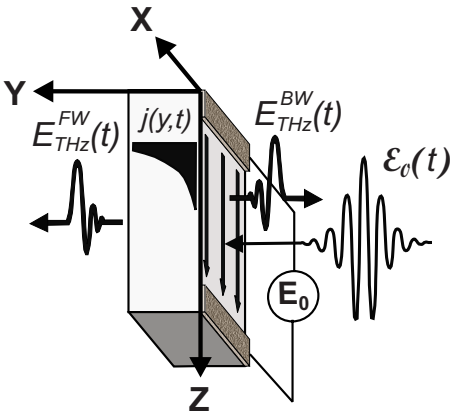

FIG. 1. (Color online) The sketch of biased semiconductor slab. The black segment shows y distribution of current $j(y,t)$ inside the slab. The gap between the bias electrodes is subjected to uniform in-plane excitation with a pump pulse field $\mathcal{E}_0(t)$. $E_{\mathrm{THz}}^{\mathrm{FW}}(t)$ and $E_{\mathrm{THz}}^{\mathrm{BW}}(t)$ show the pulses of terahertz field emitted in forward and backward directions, respectively.

II. THEORY

In what follows we consider a single semiconducting slab of a finite thickness d with dc bias field $\mathbf{E}_0$ applied to the side ohmic contacts. Nonequilibrium e-h plasma is generated in the slab under the uniform in-plane excitation of the gap between the bias electrodes. Figure 1 shows the side view of semiconducting slab, the coordinate frame, the directions of applied bias electric field, and a schematic side section view of the excitation in-depth distribution. Without loss of generality we choose the direction of EMR electric component along z axis and magnetic component along x axis. We also assume that the transient current and electric field induced in e-h plasma do not depend on x and z coordinates. It follows from the assumption of the uniform excitation of semiconductor between the bias electrodes.

A. Photocurrent in e-h plasma: Nonequilibrium Boltzmann equation approach

The photocurrent density $\mathbf{j}(y,t)$ in nonequilibrium e-h plasma created in semiconducting slab biased with an external dc electric field $\mathbf{E}_0$ is given by[26]

$$\mathbf{j}(y,t) = \frac{\hbar e}{4\pi^3}\int \mathbf{k}\left[\frac{f_{ae}(\mathbf{k},\mathbf{r},t)}{m_e} - \frac{f_{ah}(\mathbf{k},\mathbf{r},t)}{m_h}\right]d^3\mathbf{k}, \quad (1)$$

where f_{ae} and f_{ah} are the asymmetric terms of the total distribution functions for electrons, f_e, and holes, f_h, respectively, $\mathbf{k}$ is the electron wave vector, m_e and m_h are the effective masses of free carriers, electrons, and holes, respectively. In Eq. (1) we have taken into account the sign of electron charge $e=-e$. Because of commonly met material properties corresponding to the relationship $m_e \ll m_h$, we can neglect the second term in the right-hand side of Eq. (1). Then the photocurrent density in the direction of the bias field is reduced to

$$\mathbf{j}(y,t) = \frac{\hbar e}{4\pi^3}\int \mathbf{k}\frac{f_{ae}(\mathbf{k},\mathbf{r},t)}{m_e}d^3\mathbf{k}. \quad (2)$$

The total distribution function for electrons $f(\mathbf{k},\mathbf{r},t) \equiv f_e(\mathbf{k},\mathbf{r},t)$ is found from the solution of the Boltzmann equation,[26]

$$\frac{\partial f}{\partial t} + \mathbf{v}(\mathbf{k})\cdot\nabla_{\mathbf{r}} f + \frac{e\tilde{\mathbf{E}}}{\hbar}\cdot\nabla_{\mathbf{k}} f = \left(\frac{\partial f}{\partial t}\right)_{\text{col}}, \quad (3)$$

where $\tilde{\mathbf{E}}=\mathbf{E}_0+\mathbf{E}$ is the total EM field including the bias field, $\mathbf{E}_0$, and the generated EMR field, $\mathbf{E}$. The right-hand side of Eq. (3) represents the collision integral. Expanding the collision integral, $(\frac{\partial f}{\partial t})_{\text{col}}$, we obtain the following form of the nonequilibrium Boltzmann equation for photoexcited e-h plasma:[26–28]

$$\frac{\partial f}{\partial t} + \frac{\hbar\mathbf{k}}{m_e}\cdot\nabla_{\mathbf{r}} f + \frac{e}{\hbar}\tilde{\mathbf{E}}\cdot\nabla_{\mathbf{k}} f = -\Gamma(f-\tilde{f}) + I_T(f) - \gamma f + G(y,t)\frac{\pi^2\delta(k-k_0)}{k_0^2}, \quad (4)$$

where $\mathbf{v}(\mathbf{k})=\frac{\hbar\mathbf{k}}{m_e}$, $\tilde{f}$ is the distribution function averaged over angles between $\mathbf{k}$ and k_z, Γ^{-1} is collision lifetime, γ^{-1} is the lifetime of nonequilibrium carriers and electrons, $I_T(f)$ is the e-thermalization term, $G(y,t)$ is the generation term, $k_0^2 = \frac{(\hbar\omega_0 - E_g)m_e m_h}{\hbar^2(m_e+m_h)}$, E_g is the forbidden gap and ω_0 is the quantum energy of pump. At this step, without loss of generality, we make two assumptions. First, we neglect in Eq. (4) the collision integral component responsible for electron-electron collision.[26] This assumption is valid if the mean time of electron-electron collision is bigger than both the energy relaxation time and electron momentum relaxation time. Second, in order to maximize the state of nonequilibrium distribution of electrons, the lifetime of photocarriers, γ^{-1}, must be smaller than the mean time of electron-phonon relaxation, $\tau_{e\text{-ph}}$. Therefore, under the condition $\gamma^{-1} \ll \tau_{e\text{-ph}}$ we can neglect the thermalization term $I_T(f)$ in the right-hand side of Eq. (4). The used hierarchy of mean times is very typical for low-temperature grown GaAs (LTG GaAs) and the structures made of Si layer grown on sapphire (SOS): the nonequilibrium carrier lifetime reaches typically $\gamma^{-1} \simeq 0.35-0.4$ ps.[29,30] The thermalization mean time is estimated in the range of $\tau_{e\text{-ph}} \sim 10^{-12}-10^{-11}$ s.[31] The recombination rate adopted for further calculations in Eq. (4) restricts the model to the case of linear, monomolecular, and recombination laws. It is quite easy to see that this hierarchy of times corresponds to the upper limit of excitation power density $P_{\text{upper}} \sim 10^5$ W cm^{-2} for the linear recombination to remain dominant. The experimental power densities used for the excitation of e-h plasma in terahertz semiconducting emitters are normally well below this estimated upper limit. The remaining terms of the collision integral describe the processes of ballistic, drift, and diffusion motion of nonequilibrium carriers. To find the solution of the Boltzmann equation it is convenient to decompose the total nonequilibrium distribution function f into the sum of symmetric f_s and asymmetric f_a terms in $\mathbf{k}$ space. The functions f_a and f_s have the following transformation properties: $f_a(\mathbf{k},\mathbf{r},t)=-f_a(-\mathbf{k},\mathbf{r},t)$, $f_s(\mathbf{k},\mathbf{r},t)=f_s(-\mathbf{k},\mathbf{r},t)$, and $f_s=\tilde{f}$. This explains why the photocurrent in Eqs. (1) and (2) is determined only by asymmetric part of f and f_a. Then Eq. (4) splits into the set of two equations for f_a and f_s, respectively,

$$\frac{\partial f_s}{\partial t} + \frac{\hbar\mathbf{k}}{m_e}\cdot\nabla_{\mathbf{r}} f_a + \frac{e}{\hbar}\tilde{\mathbf{E}}\cdot\nabla_{\mathbf{k}} f_a = -\gamma f_s + G(y,t)\frac{\pi^2\delta(k-k_0)}{k_0^2}, \quad (5)$$

$$\frac{\partial f_a}{\partial t} + \frac{\hbar\mathbf{k}}{m_e}\cdot\nabla_{\mathbf{r}} f_s + \frac{e}{\hbar}\tilde{\mathbf{E}}\cdot\nabla_{\mathbf{k}} f_s = -\Gamma f_a - \gamma f_a. \quad (6)$$

The function f_a has two components related to diffusion and drift photocurrents. It is clear that the value of diffusion photocurrent is much weaker than that of the drift photocurrent. Even if this was not the case, the direction of diffusion photocurrent should be perpendicular to the plane of semiconducting slab, and therefore, the diffusion photocurrent would have caused the emission field with the Poynting vector lying in-plane of semiconducting slab that had no component in y direction. For these two reasons we neglect the second term in left-hand side of Eq. (5). Then, we estimate the third term in the left-hand side of Eq. (5). It is known[26,32] that function f_a is the linear one on electric field. In particular case of LTG GaAs Ohm's law behavior of I-V extends up to the bias fields $E_0 \sim 10^4$ V cm^{-1}.[33,34] In biased terahertz emitters the value of bias voltage E_0 usually remains below the above cited threshold. The requirement of I-V linearity leads to the condition $|f_a| \ll f_s$. The third term, being quadratic on $\tilde{\mathbf{E}}$, causes nonlinear dependence of photocurrent $\propto f_a^2$. This condition, for example, corresponds to heating of carriers being responsible for non-Ohmic behavior. Therefore, restricting the calculations of photocurrent to the case of the linear regime on $\tilde{\mathbf{E}}$, we should omit the third term in left-hand side of Eq. (5). Then Eq. (5) acquires the form of

$$\frac{\partial f_s}{\partial t} = -\gamma f_s + G(y,t)\frac{\pi^2\delta(k-k_0)}{k_0^2}. \quad (7)$$

The generation term $G(y,t)$ in Eq. (7) is determined by the spatiotemporal distribution of traveling pump pulse inside semiconducting slab,

$$G(y,t) = \frac{\alpha(1-R)I_0}{\hbar\omega_0}\exp(-\alpha y)\exp\left[-\frac{\left(t-\frac{y}{v_{g0}}\right)^2}{2\tau_0^2}\right], \quad (8)$$

where I_0 is the peak intensity of pump source, α and R are the absorption coefficient and reflection coefficient of semiconducting slab at the pump frequencies, respectively, and v_{g0} is the group velocity of pump pulse. Equation (8) takes into account the finite absorption of the pump pulse in the slab that leads to the nonuniform *e-h* carrier density along y axis. What is more important is that the excitation pulse in the form of Eq. (8) is not stationary in space but travels along y direction with the velocity v_{g0}. Such a traveling excitation pulse generates *e-h* plasma all the way through, depending on the value of αy. On the scale of $y < \alpha^{-1}$ this produces the effect of moving front side of the *e-h* plasma bunch or the whole bunch itself (if $\gamma^{-1} \ll t_b$) with the velocity v_{g0}. Equation (7) is solved using Fourier transform,

$$f_s(\omega) = \frac{\pi^2 G(\omega)}{k_0^2(\gamma - \imath\omega)}\exp\left(\imath\frac{\omega}{\tilde{v}_g}y\right)\delta(k-k_0), \quad (9)$$

where $\frac{1}{\tilde{v}_g} = \frac{1}{v_{g0}} + \imath\frac{\alpha}{\omega}$ is the complex group velocity and $G(\omega)$ has the form

$$G(\omega) = \frac{\alpha(1-R)I_0\tau_0}{\hbar\omega_0}\exp\left(-\frac{\omega^2\tau_0^2}{2}\right). \quad (10)$$

The asymmetric part of distribution function, f_a, is obtained from Eq. (6),

$$f_a(\omega) = -\frac{e}{\hbar}\left(\frac{1}{\gamma+\Gamma-\imath\omega}\right)(\tilde{\mathbf{E}}\cdot\nabla_{\mathbf{k}}f_s) - \frac{\hbar}{m}\left(\frac{1}{\gamma+\Gamma-\imath\omega}\right) \times(\mathbf{k}\cdot\nabla_{\mathbf{r}}f_s). \quad (11)$$

Using Eqs. (9) and (11) the integral of Eq. (2) is calculated over $\mathbf{k}$ space at the conditions $\mathbf{E} \ll \mathbf{E}_0$ and $\mathbf{E}_0 = E_{z0}\frac{\mathbf{z}}{z}$ (the bias field has only z component). After substituting Eq. (11) into Eq. (2) j_z component of the photoinduced current is given in the form,

$$j_z(\omega,y) = -\frac{e^2}{4\pi m_e}E_{0z}\frac{G(\omega)}{(\gamma-\imath\omega)(\Gamma+\gamma-\imath\omega)}\exp\left(\imath\frac{\omega}{\tilde{v}_g}y\right) \times\frac{1}{k_0^2}\int k_z\frac{\partial}{\partial k_z}[\delta(k-k_0)]d^3k. \quad (12)$$

Finally, the integration of Eq. (12) is accomplished using the relationship $\int_{\infty}^{+\infty} f(x)\delta'(x-a)dx = -f'(x)|_{x=a}$;

$$j_z(\omega,y) = \frac{e^2}{m_e}E_{0z}\frac{G(\omega)}{(\gamma-\imath\omega)(\Gamma+\gamma-\imath\omega)}\exp\left(\imath\frac{\omega}{\tilde{v}_g}y\right). \quad (13)$$

This expression for $j_z(\omega,y)$ has a form of a traveling with the complex velocity $\tilde{v}_g$ wave of nonequilibrium *e-h* plasma bunch $\propto\exp(\imath\frac{\omega}{\tilde{v}_g}y)$ in y direction carrying dissipative transverse current in the direction of applied bias in z direction. The amplitude spectrum of Eq. (13) is defined by the spectrum of excitation pulse, $G(\omega)$, and two dissipative factors related to the mean times γ^{-1} and Γ^{-1}. We emphasize the difference in functional dependence of Eq. (13) on the resistive current scattering time Γ^{-1}, lifetime of carriers γ^{-1}, and the spatial decay of excitation light beam due to absorption coefficient α.

B. Calculation of EM-fields generated by *e-h* plasma motion

Considering the excitation geometry shown in Fig. 1, we hold **E** and **H** fields dependent only on y coordinate. Then the set of Maxwell equations is

$$-\frac{\partial H_x(y,t)}{\partial y} = j(y,t) + \frac{\partial D_z(y,t)}{\partial t}, \quad (14)$$

$$\frac{\partial E_z(y,t)}{\partial y} = -\mu_0\frac{\partial H_x(y,t)}{\partial t}, \quad (15)$$

where $D_z(y,t) = \epsilon_0\int_{-\infty}^{+\infty}dt'\,\epsilon(t-t')E_z(y,t')$, $\epsilon(t)$ is the dielectric constant of semiconductor, and $j(y,t)$ is the current produced by the motion of nonequilibrium *e-h* plasma. The set of Eqs. (14) and (15) is transformed to the single equation, the wave equation, determining the field inside slab,

$$\frac{\partial^2 E_z(y,t)}{\partial y^2} - \frac{1}{c_0^2}\int_{-\infty}^{+\infty}dt'\,\epsilon(t-t')\frac{\partial^2}{\partial t'^2}E(y,t') = \mu_0\frac{\partial j_z(y,t)}{\partial t}, \quad (16)$$

where $c_0^2 = \frac{1}{\epsilon_0\mu_0}$. After applying the Fourier transform to Eq. (16) and substitution of Eq. (13) instead of $j_z(y,t)$ it takes the form of inhomogeneous Helmholtz equation,

$$\frac{d^2E_z(\omega,y)}{dy^2} + \frac{\omega^2}{c^2}E_z(\omega,y) = -\imath\frac{e^2}{m_e}\frac{\mu_0\omega G(\omega)E_{0z}}{(\gamma-\imath\omega)(\Gamma+\gamma-\imath\omega)}\exp\left(\imath\frac{\omega}{\tilde{v}_g}y\right). \quad (17)$$

where $c^2 = \frac{c_0^2}{\epsilon(\omega)}$. The general solution of inhomogeneous Helmholtz equation is the sum of the solution of homogeneous equation and a particular solution of inhomogeneous Eq. (10),

$$E_z(\omega,y) = C_1\exp\left(\imath\frac{\omega}{c}y\right) + C_2\exp\left(-\imath\frac{\omega}{c}y\right) + \tilde{\mathcal{E}}_z(\omega,y), \quad (18)$$

where C_1 and C_2 are the integration constants and $\tilde{\mathcal{E}}_z(\omega,y)$ is the particular solution of Eq. (17). The integration constants are found from the solution of boundary value problem for Eq. (18). It turns into the set of BC for **E** and **H** fields that require the continuity of tangential components of the fields across boundary. In this case they match the field in free space with the field generated inside semiconducting slab. The fields in free space are found from Eqs. (14) and (15) with $j=0$ in right-hand side of Eq. (14). The BC takes the form of

$$E_z(0-,\omega) = E_z(0+,\omega), \quad (19)$$

$$\frac{dE_z(0-,\omega)}{dy} = \frac{dE_z(0+,\omega)}{dy}, \quad (20)$$

for the front boundary and

$$E_z(d-,\omega) = E_z(d+,\omega), \tag{21}$$

$$\frac{dE_z(d-,\omega)}{dy} = \frac{dE_z(d+,\omega)}{dy}, \tag{22}$$

for the rare boundary. Equations (19) and (21) represent the BC for electric component of EMR, Eqs. (20) and (22) relate the magnetic components of EMR across the boundaries.

Here we note that previously published papers[2,12,16–18] considered terahertz emission from PCA chip on the base of idealized assumption of pure surface current inducing external terahertz EMR. The external field within this idealized scheme was calculated directly from the BC for **E** and **H** fields containing surface current without proper solution of wave equation. Such an approach, in spite of its seeming simplicity, suffers from severe drawbacks, major of which is the inconsistence of the concept of surface current with the electrodynamics of a slab with finite bulk photocurrent. To justify the choice of BC for magnetic component in the form of Eqs. (20) and (22) without inclusion of surface current term, let us consider a finite bulk current in the direction parallel to the surface with the density $j_n = \frac{dJ}{dS}$, where dJ is the bulk current flowing through a surface S. Using the notation of Fig. 1 we define $dS = dxdy$. On the other hand, the surface current is defined as a rate of charge change per unit time per unit length measured in plane in the direction perpendicular to the current flow. Then, using the notation of Fig. 1, the surface current J_S can be introduced as $J_S = \frac{dJ}{dx}$. Next, to deduce the amount of current dJ flowing through the surface element dx we send dy to zero,

$$dJ = \lim_{dy\to 0} j_n dS = \lim_{dy\to 0} j_n dxdy = 0. \tag{23}$$

It is quite clear from Eq. (23) that if the bulk current density j_n is finite, the surface current $J_S \to 0$. Therefore, at the conditions of photoexcitation of a semiconductor slab with finite value of α the BC for magnetic component of EM wave must not include the surface current term.

The particular solution $\tilde{\mathcal{E}}_z(\omega, y)$ of Eq. (17) is given in the form,

$$\tilde{\mathcal{E}}_z(\omega,y) = \mu_0 \imath\omega \frac{e^2}{\pi^2 m_e} \frac{L_{\text{form}}^{\text{FW}} L_{\text{form}}^{\text{BW}} E_{0z}}{(\gamma - \imath\omega)(\Gamma + \gamma - \imath\omega)} G(\omega) \exp\left(\imath \frac{ga}{\tilde{v}_g} y\right)$$
$$= \Xi(\omega) \exp\left(\imath \frac{\omega}{\tilde{v}_g} y\right), \tag{24}$$

where

$$\Xi(\omega) = \mu_0 \imath\omega \frac{e^2}{\pi^2 m_e} \frac{L_{\text{form}}^{\text{FW}} L_{\text{form}}^{\text{BW}} E_{0z}}{(\gamma - \imath\omega)(\Gamma + \gamma - \imath\omega)} G(\omega). \tag{25}$$

In Eqs. (24) and (25) we define the complex formation lengths for backward and forward emitted radiation,

$$\tilde{L}_{\text{form}}^{\text{BW/FW}}(\omega) = \frac{\pi}{\frac{\omega}{\tilde{v}_g}\left(1 \pm \frac{\tilde{v}_g}{c}\right)}, \tag{26}$$

with the signs "–" and "+" in the denominator corresponding to the EMR emitted by a moving source into forward (FW) and backward (BW) hemispheres $\{-\pi/2, \pi/2\}$, respectively. The continuity of **E** and **H** fields at the interfaces $y=0$ and $y=d$, Eqs. (19)–(22) determine the radiation propagating outwardly from the slab, in forward and backward directions, respectively. To fulfill the BC, we match the general solution describing the electric component inside the slab;

$$E_z(y,\omega) = C_1 \exp\left(\imath \frac{\omega}{c} y\right) + C_2 \exp\left(-\imath \frac{\omega}{c} y\right)$$
$$+ \Xi(\omega) \exp\left(\imath \frac{\omega}{\tilde{v}_g} y\right), \tag{27}$$

with the solutions of the wave equation in free space on both sides of the slab. Terahertz field $E_z(y,\omega)$ irradiated backward into the left-hand half of free space at $y<0$,

$$E_z(y,\omega) = C_{\text{BW}} \exp\left(-\imath \frac{\omega}{c_0} y\right). \tag{28}$$

Forward irradiated terahertz field $E_z(y,\omega)$ into the right-hand half of free space at $y>d$,

$$E_z(y,\omega) = C_{\text{FW}} \exp\left[\imath \frac{\omega}{c_0}(y-d)\right]. \tag{29}$$

The values of the integration constants, $C_1 \equiv C_1(\omega)$, $C_2 \equiv C_2(\omega)$, $C_{\text{BW}} \equiv C_{\text{BW}}(\omega)$, and $C_{\text{FW}} \equiv C_{\text{FW}}(\omega)$ are determined from the BC for the tangential components of **E** and **H** fields. The conservation of the tangential components Eqs. (19)–(22) leads to the following set of linear equations represented in matrix form as

$$\begin{pmatrix} 1 & 1 & -1 & 0 \\ \frac{1}{c} & -\frac{1}{c} & \frac{1}{c_0} & 0 \\ \exp\left(\imath \frac{\omega}{c} d\right) & \exp\left(-\imath \frac{\omega}{c} d\right) & 0 & -1 \\ \frac{1}{c}\exp\left(\imath \frac{\omega}{c} d\right) & -\frac{1}{c}\exp\left(-\imath \frac{\omega}{c} d\right) & 0 & -\frac{1}{c_0} \end{pmatrix} \otimes \begin{pmatrix} C_1 \\ C_2 \\ C_{\text{BW}} \\ C_{\text{FW}} \end{pmatrix}$$
$$= -\Xi \cdot \begin{pmatrix} 1 \\ \frac{1}{\tilde{v}_g} \\ \exp\left(\imath \frac{\omega}{\tilde{v}_g} d\right) \\ \frac{1}{\tilde{v}_g}\exp\left(\imath \frac{\omega}{\tilde{v}_g} d\right) \end{pmatrix}, \tag{30}$$

The solution of this matrix equation gives the values of integration constants (the details are given in Ref. 5). The complex amplitudes for the forward and backward emitted

terahertz fields outside the slab are given by the pre-exponential factors of Eqs. (28) and (29), respectively,

$$E_z(d+,\omega) = -\frac{c_0}{\tilde{v}_g}\frac{\Xi(\omega)}{(c-c_0)^2\exp(\imath\omega d/c)-(c+c_0)^2\exp(-\imath\omega d/c)}\{(c+c_0)(c+\tilde{v}_g)\exp[-\imath\omega d(1/c-1/\tilde{v}_g)] - (c-c_0)(c-\tilde{v}_g)\exp[\imath\omega d(1/\tilde{v}_g+1/c)]-2c(\tilde{v}_g+c_0)\}, \quad (31)$$

$$E_z(0-,\omega) = +\frac{c_0}{\tilde{v}_g}\frac{\Xi(\omega)}{(c-c_0)^2\exp(\imath\omega d/c)-(c+c_0)^2\exp(-\imath\omega d/c)}\{2c(\tilde{v}_g-c_0)\exp(\imath\omega d/\tilde{v}_g)+(c+c_0)(c-\tilde{v}_g)\exp(-\imath\omega d/c) - (c+\tilde{v}_g)(c-c_0)\exp(\imath\omega d/c)\}, \quad (32)$$

where the notations $z=d+$ and $z=0-$ show the coordinates outside the slab, respectively. The solutions Eqs. (31) and (32) converge to zero if the thickness of photoconductive material $d\to 0$. They describe the field distributions at the output aperture that is used to find the field in a remote zone far from the slab. Equations (31) and (32) can be transformed into the following expressions that are more suitable for qualitative analysis. The field on the outer aperture of the rare slab boundary producing forward emitted terahertz EMR takes the form of

$$E_z(d+,\omega) = -t\frac{c_0\tilde{\Xi}(\omega)}{1-r^2\exp\left(\imath\frac{2\omega d}{c}\right)}\left\{\left[\frac{1}{2(1-\imath\omega\tau_{\delta n})}+\frac{r}{2(1-\imath\omega\tau_N)}\right]\exp\left(\imath\frac{\omega d}{c}\right) - \frac{1}{2(1-\imath\omega\tau_{\delta n})}\exp\left(\imath\frac{\omega\tilde{n}d}{c_0}\right) - \frac{r}{2(1-\imath\omega\tau_N)}\exp\left[\imath\frac{\omega(\tilde{n}+2n)d}{c_0}\right]\right\}. \quad (33)$$

The field on the outer aperture producing backward irradiated terahertz EMR of the front slab boundary is converted into

$$E_z(0-,\omega) = -t\frac{c_0\tilde{\Xi}(\omega)}{1-r^2\exp\left(\imath\frac{2\omega d}{c}\right)}\left\{\frac{1}{2(1-\imath\omega\tau_N)}+\frac{r}{2(1-\imath\omega\tau_{\delta n})}\exp\left(\imath\frac{2\omega d}{c}\right)-\left[\frac{1}{2(1-\imath\omega\tau_{\delta n})}+\frac{r}{2(1-\imath\omega\tau_N)}\right]\exp\left[\imath\frac{\omega(\tilde{n}+n)d}{c_0}\right]\right\}, \quad (34)$$

where $n=\sqrt{\epsilon}$, $\tilde{n}=\frac{c_0}{\tilde{v}_g}$, $r=\frac{n-1}{n+1}$, and $t=1-r$. The parameters τ_N and $\tau_{\delta n}$ have the meaning of the sum of and difference between phase and group delay times on the scale of the mean absorption length α^{-1}: $\tau_N=\frac{1}{\alpha}(\frac{1}{c}+\frac{1}{v_{g0}})$ and $\tau_{\delta n}=\frac{1}{\alpha}(\frac{1}{v_{g0}}-\frac{1}{c})$. The term $\tilde{\Xi}(\omega)$ in Eqs. (33) and (34) is given by

$$\tilde{\Xi}(\omega) = \mu_0\frac{e^2}{\pi^2 m_e}\frac{\tau_R\tau\alpha^{-1}E_{0z}}{(1-\imath\omega\tau_R)(1-\imath\omega\tau)}G(\omega). \quad (35)$$

where $\tau_R=(\gamma+\Gamma)^{-1}$ and $\tau=\gamma^{-1}$. The common factor t in Eqs. (33) and (34) accounts for the transmission of the fields across the boundary "semiconductor air." The inverse Fourier transform of Eqs. (33) and (34) returns the time domain waveforms of terahertz field within the aperture S_0 on the outer surfaces of semiconducting slab.

The spatial distribution of terahertz EMR emitted into free space from the input and output surfaces of a nonlinear slab can be treated within the framework of the standard diffraction theory.[35] The active volume of e-h plasma inside the slab forms a small cylinder with the apertures on both input and output surfaces of the order of $\sim S_0$, where S_0 is the pump beam cross section. The scalar term $E_x(r,\omega)$ of terahertz field at an observation point r in free space behind the slab is found after solving the integration,

$$E_z^{\mathrm{FW}}(r,\omega) = \frac{\imath\omega}{2\pi c_0}\int_{S_0}E_z(d+,\omega)\frac{\exp(\imath kr)}{r}\cos(\mathbf{n},\mathbf{r})dS_0, \quad (36)$$

where $E_x(d+,\omega)$ is the field at the output aperture calculated from Eq. (33). The integral in Eq. (36) is taken over the pump/terahertz beam aperture cross section S_0. The time domain waveform $E_x(\mathbf{r},t)$ is obtained from Eq. (36) using the Fourier transform. The field waveform at the distance r from the slab is given by

$$E_{\mathrm{THz}}^{\mathrm{FW}}(t) = E_x^{\mathrm{FW}}(r,t) = \frac{1}{(2\pi)^2 c_0}\int_{S_0}\frac{\cos(\mathbf{n},\mathbf{r})}{r}\frac{d}{dt}E_z\left(d+,t-\frac{r}{c_0}\right)dS_0. \quad (37)$$

Similarly, the terahertz field emitted by the slab in the backward direction, $E_{\mathrm{THz}}^{\mathrm{BW}}(t)$, is found from Eqs. (34) and (35) using $E_z(0-,\omega)$ instead of $E_z(d+,\omega)$.

III. DISCUSSION

Both Eqs. (33) and (34) are given by the sum of several terms, each of the terms corresponding to the partial pulse component associated with the generation mechanisms and

spatial dependencies of EMR formation. The complexity of Eqs. (33) and (34) differs in nature from the simplest elementary models based on the representation of a single radiative dipole, surface current, or a small localized photoexcited spot embedded in a dielectric medium hold between the bias contacts and used in previous publications.[12–24] Below we review the role of each partial term in Eqs. (33) and (34), describing their nature and criteria under which the contribution of the term becomes essential. We start the discussion from Eq. (34), describing backward emitted terahertz field.

The factor $\tilde{\Xi}(\omega)$ represents the isotropic part of the spectrum of terahertz EMR pulse generated by moving bunch of *e-h* plasma inside the slab. It is modulated by the Fabry-Perot factor $[1-r^2\exp(\imath\frac{2\omega d}{c})]^{-1}$ describing multiple reflections of terahertz pulse between slab's boundaries. The other important factor affecting further broadening of terahertz EMR pulse is the sum of terms in curly braces in Eq. (33) or (34), whose form depends on the emission direction. We shall see that terahertz pulses consists of several components with different delay times related to the location of radiation events and direction of radiation. Let us turn to the analysis of these directional terms.

We consider first the directional term of Eq. (34) describing terahertz field emitted backward. The first term in the curly braces, $\propto\frac{1}{2(1-\imath\omega\tau_N)}$, does not possess any delay-time factor, and therefore, it corresponds to the first pulse in time scale to arrive at the observer's position at a far-field zone. The spectrum of this component is determined by the relaxation due to the mean time τ_N representing the sum of the transit time for terahertz EMR and excitation pulses propagating the distance α^{-1}, respectively.

The second term, $\frac{r}{2(1-\imath\omega\tau_{\delta n})}\exp(\imath\frac{2\omega d}{c})$, represents the pulse delayed against the first pulse component by $\Delta t_{2\mathrm{BW}}=\frac{2d}{c}$. The value of $\Delta t_{2\mathrm{BW}}$ corresponds to the round trip time of terahertz pulse emitted from the front boundary and propagating to the rare boundary and backward. The spectral content of this term depends on the relaxation with the mean time $\tau_{\delta n}$ that is the difference of transit times for terahertz and excitation pulses crossing the distance α^{-1}. The amplitude of this term and its spectral content also depends on the reflection coefficient r at the rare boundary of the slab.

The third term represented by the sum of two items in square brackets of Eq. (34) becomes significant at the conditions of moderate absorption, $\alpha d\sim 1$. Its delay time is $\Delta t_{3\mathrm{BW}}=\frac{d}{\tilde{v}_g}+\frac{d}{c}$ with reference to the first pulse component. The first item of $\Delta t_{3\mathrm{BW}}$, $\frac{d}{\tilde{v}_g}$, corresponds to the time needed for the moving source to reach the rare boundary and the second item $\frac{d}{c}$ is the single transit time for terahertz pulse. The said unequivocally shows that this pulse emanates from the rare surface of the slab where *e-h* plasma extinct due to exit of pump pulse from the slab (we do not consider the multiple reflections of pump pulse). The first item in square brackets of Eq. (34) describes the component generated in backward direction. The second item is attributed to the component generated forwardly and is immediately reflected in backward direction. The spectral content of the third term is related to the sum of two relaxation terms with the mean time $\tau_{\delta n}$ and τ_N. We note that the sign of the third term is opposite to that of the first and second terms that supports the difference in generation mechanisms of terahertz pulse at the moment of creation and extinction of *e-h* plasma at the condition $\alpha d\lesssim 1$.

A similar analysis is carried out for the directional term in curly braces of Eq. (33), which describes the terahertz pulse emitted from semiconducting slab in forward direction. The first term in the square brackets $\frac{1}{2(1-\imath\omega\tau_{\delta n})}$ represents direct forward emission, while $\frac{r}{2(1-\imath\omega\tau_N)}$ corresponds to the wave backwardly emitted and subsequently reflected in the forward direction. Both components propagate together from the front boundary across the slab. Hence, is the common delay time $\Delta t_{1\mathrm{FW}}=\frac{d}{c}$. The sum of two relaxation terms with the mean times $\tau_{\delta n}$ and τ_N has effect on the spectrum of this component.

The second and the third components are effectively generated at conditions $\alpha d\lesssim 1$. The second component has the delay time $t_{2\mathrm{FW}}=\frac{d}{\tilde{v}_g}$, which proves that it is radiated from the rare boundary. The spectrum of this pulse is characterized by the relaxation term $\propto\frac{r}{2(1-\imath\omega\tau_{\delta n})}$. The third component has the delay $t_{3\mathrm{FW}}=\frac{d}{\tilde{v}_g}+\frac{2d}{c}$, where the first item of the delay $\propto\frac{d}{\tilde{v}_g}$ corresponds to the time for excitation pulse to propagate across the sample and generate terahertz pulse at the rare boundary and the second item of the delay $\propto\frac{2d}{c}$ represents the round trip time of terahertz pulse. It demonstrates that this component is emitted from the rare boundary in backward direction and bounces from the front boundary back in forward direction. The spectrum of this component is described by the relaxation term $\propto\frac{r}{2(1-\imath\omega\tau_N)}$. Similar to Eq. (34) the signs of the second and third components are opposite to that of the first component due to the difference in generation mechanisms of terahertz pulse at the moment of creation and extinction of *e-h* plasma at $\alpha d\lesssim 1$.

For numerical calculations and graphical presentations of terahertz spectra Eqs. (31)–(37) we use the following expression for the lattice contribution in the dielectric constant $\epsilon(\nu)$ of a polar material:[36]

$$\frac{\epsilon(\nu)}{\epsilon_0}=\kappa_\infty+\frac{\nu_{TO}^2(\kappa_0-\kappa_\infty)}{\nu_{TO}^2-\nu^2+\imath\gamma_p\nu}, \tag{38}$$

where $\kappa_0=\kappa_\infty(\frac{\nu_{LO}}{\nu_{TO}})^2$. The dielectric constant for a nonpolar semiconductor (e.g., Si) can be evaluated using $\frac{\epsilon(\nu)}{\epsilon_0}=\kappa_0$. The values of material parameter, γ_p, n, and α and effective masses for GaAs and Si were taken from Refs. 36–40, respectively. We do not include Eq. (38) into the calculations of terahertz waveforms keeping $\epsilon(\nu)=\epsilon_0$ in order to smoothen out the waveforms removing the oscillations introduced by phonon peaks in $\epsilon(\nu)$ Eq. (38).

Figure 2 plots several calculated terahertz waveform emitted backward from a semiconducting slab of different thicknesses, $\gamma^{-1}=1\times10^{-12}$ s, $\Gamma^{-1}=1.7\times10^{-13}$ s, and $\alpha=200$ cm^{-1}. To develop the full time-of-flight content of terahertz pulse we choose the value of α corresponding to the case $\alpha d\lesssim 1$. In order to remove the replicas related to multiple reflections of generated terahertz pulse we calculate the waveforms of Fig. 2 for a semiconducting slab immersed in a medium with the refractive index equal to that of semi-

conducting slab at terahertz frequencies. Chosen material parameters are typical for Si, which is used in SOS PCA at $\lambda = 950$ Å. The amplitude and time position of the first pulse remains independent of d. This shows that the generation of terahertz pulse occurs at the front surface of semiconducting slab where nonequilibrium e-h plasma is generated. The front edge of the second pulse (marked with arrows), having the sign opposite of the first pulse, shifts linearly with the change in slab's thickness with the amplitude decreasing with thickness. The time shift of the second pulse front varies as $\propto \frac{d}{\tilde{v}_g} + \frac{d}{c}$—the inset of Fig. 2. This evidence proves that the second pulse is generated with the delay required for e-h plasma to reach the rare boundary and extinct there due to pump pulse exit from the rare surface of semiconducting slab. Figure 2 exhibits convincing demonstration of a close analogy of the generation of twin pulse terahertz EMR in this case with the phenomena of nonlinear optic wave interactions reported in Ref. 4 and elaborated in details in Ref. 5. In the treatment of both problems the source term of inhomogeneous Helmholtz equation in the form of Eq. (17) represents a uniformly propagating source described by the factor $\propto \mathcal{A}(\omega)\exp(\imath \frac{\omega}{v_g} y)$, where v_g is the group velocity of pump pulse and y is the propagation coordinate. The amplitude of the source described by pre-exponential factor, $\mathcal{A}(\omega)$, is given by

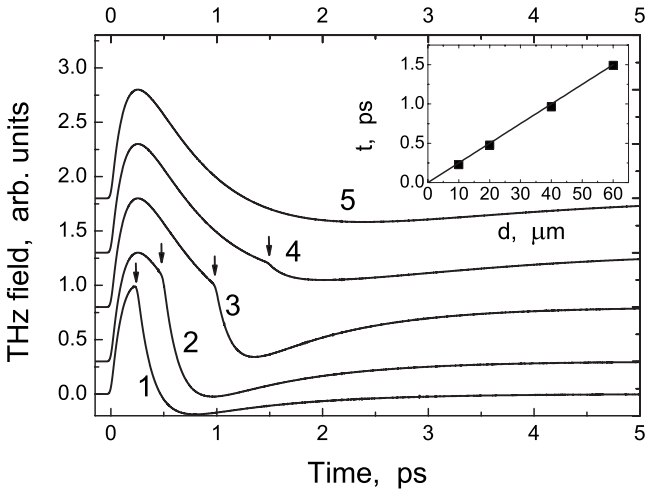

FIG. 2. Calculated waveforms of terahertz field emitted in backward direction from biased semiconductor slab. The waveforms correspond to different thicknesses shown in the inset: $d=10$ (curve 1), 20 (curve 2), 40 (curve 3), and 60 μm (curve 4), respectively; curve 5 is calculated for $\alpha d=3$. The inset: solid squares shows the time positions of the second pulse front edge and solid line, time dependence $t=\frac{d}{\tilde{v}_g}+\frac{d}{c}$.

$$\mathcal{A}(\omega) \propto \begin{cases} \omega^2 \exp\left(-\dfrac{\omega^2 \tau_0^2}{2}\right), & \text{nonlinear optical conversion} \\ \dfrac{\omega}{(\gamma - \imath\omega)(\gamma + \Gamma - \imath\omega)} \exp\left(-\dfrac{\omega^2 \tau_0^2}{2}\right), & \text{moving } e\text{-}h \text{ plasma current,} \end{cases} \tag{39}$$

for nonlinear optical conversion and current carrying or polarized e-h plasma, respectively. In the case of nonlinear optic wave conversion the frequency dependence of the amplitude $\mathcal{A}(\omega)$ is related to the Fourier transform of the second derivative term of nonlinear coupling of optic fields. Nonlinear coupling of traveling pump fields is the necessary and sufficient condition for formation of uniformly moving polarization charge.[4,5] Dissipationless nature of this polarization charge motion is entirely described as a moving wave packet. In the case of moving bunch of nonequilibrium carrying current e-h plasma the frequency spread of the source wave packet also depends on moving wave packet Eqs. (8) and (10). The factor $\propto\omega$ comes from the Fourier transform of the first derivative of transverse current. In addition $\mathcal{A}(\omega)$ has a product of two relaxation factors, $(\gamma-\imath\omega)^{-1}(\gamma+\Gamma-\imath\omega)^{-1}$ in Eq. (39), related to the dissipations of transverse current. In both cases of Eq. (39) the source uniformly propagates with the velocity of pump wave. The predicted new effect of twin terahertz pulse generation by moving bunch of nonequilibrium e-h plasma carrying transverse current in the limit of $\alpha d \lesssim 1$, likewise nonlinear optic generation of terahertz pulses,[4,5] has close analogy with the radiation phenomenon at start-stop motion of a charged particle in homogeneous media, which has been introduced and considered earlier by Tamm.[41] In the case of moving plasma bunch the necessary condition for radiation to occur is bias dc field E_{0z}. The role of bias is to induce directional ordering of carriers, transverse current, or polarization (in this paper we do not consider in details this second option, creation of polarization charge at strongly nonuniform excitation, e.g., excitation to a small focal spot whose diameter is much smaller than the gap between contacts[42]). The creation and extinction events of such uniformly moving photoinduced current or polarization in a dispersive medium with $c \neq \tilde{v}_g$ lead to the radiation of twin terahertz EM pulses.[43]

Now we turn to the estimation of terahertz pulse bandwidth—Figs. 3 and 4. The factor $\tilde{\Xi}(\omega)$ itself is constructed from the product of three Fourier transform: the excitation pulse spectrum $G(\omega)$, the first dissipation factor described by the mean time $\tau_R=(\gamma+\Gamma)^{-1}$, and the second relaxation factor related to $\tau=\gamma^{-1}$. It is normally expected that the lifetime of e-h carriers γ^{-1} exceeds the collision lifetime Γ^{-1}. Because of multiplicative form of $\tilde{\Xi}(\omega)$ the

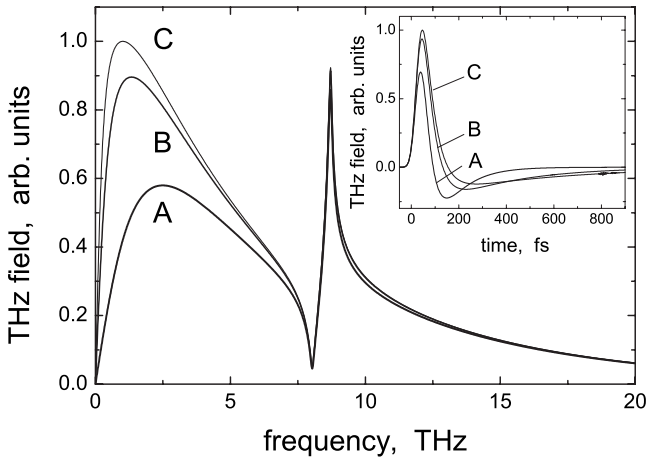

FIG. 3. Calculated spectra of terahertz radiation emitted in backward direction from biased semiconductor slab. The spectra correspond $\gamma^{-1}=100$ (curve A), 300 (curve B), and 500 fs (curve C). The spectra are calculated using the following parameters: $\tau_0=15$ fs, $\Gamma^{-1}=50$ fs, and $d=300$ μm. The inset: calculated waveforms of terahertz field emitted in backward direction from biased semiconductor slab. The contribution from the phonon resonances in Eq. (38) is replaced by $\epsilon(\omega)=\epsilon_0$ to smoothen the curves. The waveforms correspond $\gamma^{-1}=100$ (curve A), 300 (curve B), and 500 fs (curve C). The waveforms are calculated for the following parameters: $\Gamma^{-1}=50$ fs, $\tau=15$ fs, and $d=300$ μm.

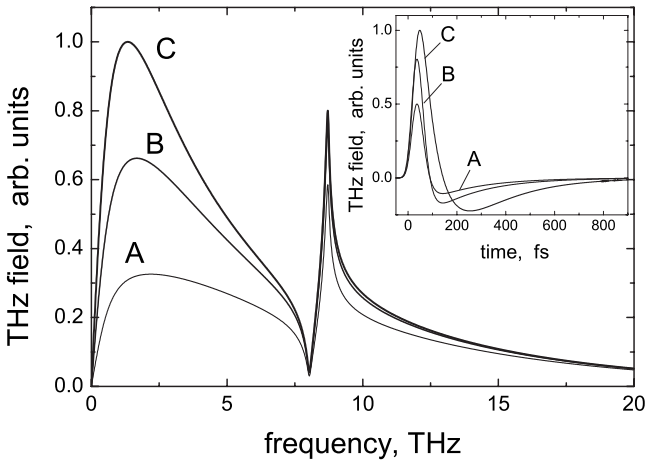

FIG. 4. Calculated spectra of terahertz radiation emitted in backward direction from biased semiconductor slab. The spectra correspond $\Gamma^{-1}=20$ fs (curve A), 50 (curve B), and 100 fs (curve C). The spectra are calculated for the following parameters: $\gamma^{-1}=200$ fs, $\tau=15$ fs, and $d=300$ μm. The inset: calculated waveforms of terahertz field emitted in backward direction from biased semiconductor slab. The contribution from the phonon resonances in Eq. (38) is replaced by $\epsilon(\omega)=\epsilon_0$ to smoothen the curves. The waveforms correspond $\Gamma^{-1}=20$ (curve A), 50 (curve B), and 100 fs (curve C). The waveforms are calculated for the following parameters: $\gamma^{-1}=200$ fs, $\tau=15$ fs, and $d=300$ μm.

spectrum of $\tilde{\Xi}(\omega)$ is restricted at high-frequency side by the complex combination of three factors: $\tilde{\Xi}(\omega)\propto G(\omega)(1-\imath\omega\tau_R)^{-1}(1-\imath\omega\tau)^{-1}$. One more factor affecting the pulse bandwidth is determined by the directional terms in curl brackets of Eqs. (33) and (34). The characteristic behavior of a dissipative term with time τ^* is described by

$$\left|(1-\imath\omega\tau^*)^{-1}\right|=\begin{cases}1, & \text{if } \omega\tau^*\ll 1\\ \dfrac{1}{\omega\tau^*} & \text{if } \omega\tau^*\gg 1,\end{cases} \tag{40}$$

where τ^* represents one of τ_R, τ, τ_N, or $\tau_{\delta n}$. The frequency spectrum of terahertz pulse emitted in forward direction at high frequencies, $\omega>\max\{\tau_R^{-1},\tau^{-1},\tau_{\delta n}^{-1}\}$, $E_z^{\mathrm{FW}}(r,\omega)$, is given by

$$E_z^{\mathrm{FW}}(r,\omega)\propto\omega\exp\left(-\frac{\omega^2\tau_0^2}{2}\right)\frac{1}{(\omega\tau_R)(\omega\tau)(\omega\tau_{\delta n})}, \tag{41}$$

whereas the high-frequency part of terahertz pulse spectrum emitted in backward direction at $\omega>\max\{\tau_R^{-1},\tau^{-1},\tau_N^{-1}\}$ $E_z^{\mathrm{BW}}(r,\omega)$, is described by

$$E_z^{\mathrm{BW}}(r,\omega)\propto\omega\exp\left(-\frac{\omega^2\tau_0^2}{2}\right)\frac{1}{(\omega\tau_R)(\omega\tau)(\omega\tau_N)}. \tag{42}$$

It is seen that the spectrum of terahertz pulse at low frequencies, $\omega<\min\{\tau_R^{-1},\tau^{-1},\tau_{\delta n}^{-1}\}$, is entirely determined by $G(\omega)$. At high frequency the spectrum is affected by the product of dissipation factors, each $\propto\frac{1}{\omega\tau^*}$, whose strong narrowing of bandwidths is demonstrated by Figs. 3 and 4. We note that the spectral bandwidth similarly responses on the variations of both γ and Γ in accordance with Eqs. (41) and (42). The factors $(\omega\tau_{\delta n})^{-1}$ and $(\omega\tau_N)^{-1}$ relate the spectral narrowing due to directional factors to the mean formation length, the spatial scales characterizing the separation of radiation, and Coulomb fields expressed by Eq. (26). The characteristic scale of the formation length in the case of terahertz EMR from moving nonequilibrium *e-h* plasma bunch in a semiconductor differs from the definition of the formation length used in the theory of radiation phenomena of moving charges[44] and at nonlinear wave conversion in weakly absorbing crystals.[4,5] If the absorption coefficient is sufficiently high, $\alpha\gg\omega(\frac{1}{v_g}\pm\frac{1}{c})=\frac{\pi}{L_{\mathrm{form}}^{\mathrm{BW/FW}}}$, the formation length is restricted down to the scale of $\pi\alpha^{-1}$ regardless the difference between v_g and c. To some extent this could be considered as an equivalent of a stationary immobile source. In the opposite case, $\alpha\ll\omega(\frac{1}{v_g}\pm\frac{1}{c})$, the formation length is given by $L_{\mathrm{form}}^{\mathrm{BW/FW}}$, respectively, for backward and forward directions, respectively.

As it follows from Eqs. (41) and (42) the input factor driving terahertz pulse bandwidth is the spectral content of pump laser pulse $G(\omega)\propto\exp(-\frac{\omega^2\tau_0^2}{2})$—Figs. 5 and 6. It is seen that even having the amplitude cutoff due to the dissipation factors associated with the material relaxation times, τ^*, a wide band of terahertz spectrum can still be achieved with a narrow pump laser pulse of ~10–30 fs although with a reduced amplitude. This trend follows from the comparison of the curves A, B, and C in Figs. 5 and 6.

Finally, we emphasize on a peculiar velocity matching property of generation terahertz pulse using moving bunch of nonequilibrium *e-h* plasma. If the conditions of velocity match are approached, $c\to v_g$, the value of $\tau_{\delta n}\to 0$. Then the

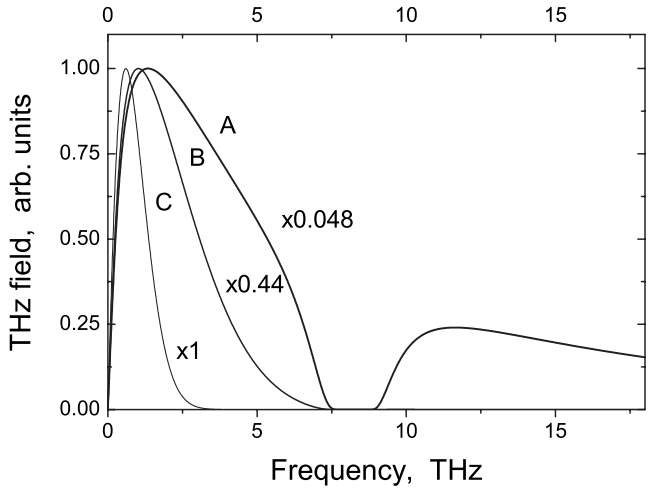

FIG. 5. Calculated spectra of terahertz radiation emitted in forward direction from biased semiconductor slab. The spectra correspond $\tau_0=10$ (curve A), 100 (curve B), and 300 fs (curve C). The spectra are calculated using the following parameters: $\gamma^{-1}=300$ fs, $\Gamma^{-1}=50$ fs, and $d=300$ μm.

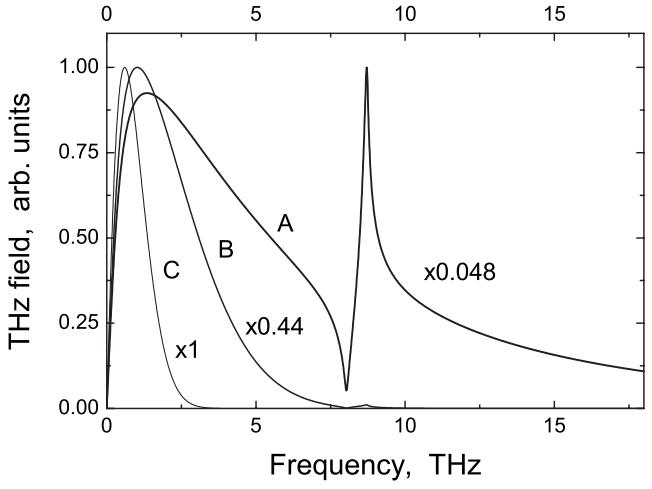

FIG. 6. Calculated spectra of terahertz radiation emitted in backward direction from biased semiconductor slab. The spectra correspond $\tau_0=10$ (curve A), 100 (curve B), and 300 fs (curve C). The spectra are calculated using the following parameters: $\gamma^{-1}=300$ fs, $\Gamma^{-1}=50$ fs, and $d=300$ μm.

relaxation factor associated with $\tau_{\delta n}$ cuts off the emission spectrum in collinear forward direction at frequencies $\omega \gtrsim \tau_{\delta n}^{-1}$ that could be too high for the dissipation due to $\tau_{\delta n}$ to become measurable. In this regard, the smaller is the value of $\tau_{\delta n}$ the higher value returns for the frequency cutoff. At the same time this condition does not affect the bandwidth of terahertz pulse emitted backward because the formation length $\tilde{L}_{\text{form}}^{\text{BW}} \propto (c+\tilde{v}_g)^{-1}$ always remains finite and small. It is seen that the spectral properties of terahertz EM radiation generated at the velocity match conditions with nonlinear optic wave conversion and by moving bunch of nonequilibrium *e-h* plasma are alike.

IV. CONCLUSIONS

To summarize, the reported theoretical results unequivocally establish the mechanism of terahertz emission applied to the most often used practical case of semiconducting biased terahertz emitter made as a PCA chip subject to the transverse (against the direction of the pump beam) bias. The first-principles calculations based on the solutions of nonequilibrium Boltzmann equation and Maxwell equations take into account the important effect of moving bunch of nonequilibrium *e-h* plasma carrying transverse current. It predicts two effect: twin terahertz EM pulse generation in the limit of $\alpha d \lesssim 1$ and the enhancement of terahertz emission at high frequencies at the velocity matching conditions. It has shown that the effect of bias voltage on *e-h* plasma is in induction of transverse current or polarization. The creation and extinction events of such uniformly moving photoinduced current or polarization source in a dispersive medium with $c \neq \tilde{v}_g$ lead to the radiation of twin terahertz EM pulses. It convincingly demonstrates a close analogy with the class of radiation phenomena considered within the framework of Tamm problem and caused by the start stop of uniform motion of a charged or polarized source in a homogeneous medium. If the conditions $\alpha d \gg 1$ are met, then the formation length for terahertz generation is restricted to the scale of $\pi\alpha^{-1}$ regardless the difference between v_g and c, showing similarity of this case to the radiation by a stationary immobile source. For both cases the presented theory has revealed the particular roles of the key material parameters: the dissipation times, γ^{-1} and Γ^{-1}, the carrier collision and decay times; the details responsible for formation of spectral content of terahertz pulse, the role of phase matching, and the influence of directional factors and excitation pulse duration on the spectrum of terahertz pulse.

ACKNOWLEDGMENTS

The authors would like to acknowledge financial support the Russian Foundation for Basic Research (Grant No. 08-02-00162) and a grant for innovations support from the Russian Academy of Sciences.

*nick.zinovev@durham.ac.uk

[1] T. Brabec and F. Krausz, Rev. Mod. Phys. **72**, 545 (2000).
[2] J. Shan and T. F. Heinz, Top. Appl. Phys. **92**, 1 (2004).
[3] M. Tonouchi, Nat. Photonics **1**, 97 (2007).
[4] N. N. Zinov'ev, A. S. Nikoghosyan, and J. M. Chamberlain, Phys. Rev. Lett. **98**, 044801 (2007).
[5] N. N. Zinov'ev, A. S. Nikoghosyan, R. A. Dudley, and J. M. Chamberlain, Phys. Rev. B **76**, 235114 (2007).

[6] X.-C. Zhang and D. H. Auston, J. Appl. Phys. **71**, 326 (1992).
[7] T. Dekorsy, H. Auer, H. J. Bakker, H. G. Roskos, and H. Kurz, Phys. Rev. B **53**, 4005 (1996).
[8] W. van Roosbroeck, Phys. Rev. **101**, 1713 (1956).
[9] J. R. Dixon, Phys. Rev. **107**, 374 (1957).
[10] K. J. Chau and A. Y. Elezzabi, Opt. Commun. **242**, 295 (2004).
[11] M. B. Johnston, D. M. Whittaker, A. Corchia, A. G. Davies, and E. H. Linfield, Phys. Rev. B **65**, 165301 (2002).
[12] D. H. Auston, K. P. Cheung, and P. R. Smith, Appl. Phys. Lett. **45**, 284 (1984).
[13] G. Mourou, C. V. Stancampiano, A. Antonetti, and A. Orszag, Appl. Phys. Lett. **39**, 295 (1981).
[14] N. Katzenellenbogen and D. Grischkowsky, Appl. Phys. Lett. **58**, 222 (1991).
[15] S. E. Ralph and D. Grischkowsky, Appl. Phys. Lett. **59**, 1972 (1991).
[16] J. T. Darrow, X.-C. Zhang, and D. H. Auston, IEEE J. Quantum Electron. **28**, 1607 (1992).
[17] P. K. Benicewicz, J. P. Roberts, and A. J. Taylor, J. Opt. Soc. Am. B **11**, 2533 (1994).
[18] S.-G. Park, A. M. Weiner, M. R. Melloch, C. W. Siders, J. L. W. Siders, and A. J. Taylor, IEEE J. Quantum Electron. **35**, 1257 (1999).
[19] P. Uhd Jepsen, R. H. Jacobsen, and S. R. Keiding, J. Opt. Soc. Am. B **13**, 2424 (1996).
[20] Z. Piao, M. Tani, and R. Sakai, Jpn. J. Appl. Phys., Part 1 **39**, 96 (2000).
[21] H. Němec, A. Pashkin, P. Kuzel, M. Khazan, S. Schnüull, and I. Wilke, J. Appl. Phys. **90**, 1303 (2001).
[22] M. Tani, M. Hermann, and K. Sakai, Meas. Sci. Technol. **13**, 1739 (2002).
[23] E. Castro-Camus, J. Lloyd-Hughes, and M. B. Johnston, Phys. Rev. B **71**, 195301 (2005).
[24] A. V. Kuznetsov and C. J. Stanton, Phys. Rev. B **48**, 10828 (1993).
[25] Strictly speaking, the representation of external field as the second time derivative of an oscillating dipole is valid only for a fixed point dipole element. In fact, the treatments of terahertz emitters based on nonequilibrium carriers transport (ambipolar diffusion or drift) require the use of full set of Maxwell and transport equations with the correct set of boundary conditions. It is clear that replacement of this detailed analysis with a point dipole or current source is inadequate in the sense of quantitative analysis.
[26] L. D. Landau and E. M. Lifshitz, *Physical Kinetics* (Pergamon, Oxford, 1991).
[27] H. J. Stocker and H. Kaplan, Phys. Rev. **150**, 619 (1966).
[28] V. I. Belinicher and S. M. Ryvkin, Zh. Eksp. Teor. Fiz. **81**, 353 (1981) [Sov. Phys. JETP **54**, 190 (1981)].
[29] K. Zhang and D. L. Miller, J. Electron. Mater. **22**, 1433 (1993).
[30] C. Kadow, S. B. Fleischer, J. P. Ibbetson, J. E. Bowers, and A. C. Gossard, Appl. Phys. Lett. **75**, 2575 (1999).
[31] I. Vurgaftman, Y. Lam, and J. Singh, Phys. Rev. B **50**, 14309 (1994).
[32] M. Lundstrom, *Fundamentals of Carrier Transport* (Cambridge University Press, Cambridge, 2000).
[33] J. P. Ibbetson and U. K. Mishra, Appl. Phys. Lett. **68**, 3781 (1996).
[34] H. Ruda and A. Shik, Phys. Rev. B **63**, 085203 (2001).
[35] M. Born and E. Wolf, *Principles of Optics* (Pergamon, New York, 1970).
[36] J. S. Blakemore, J. Appl. Phys. **53**, R123 (1982).
[37] M. Nagai and K. Tanaka, Appl. Phys. Lett. **85**, 3974 (2004).
[38] D. D. Sell, H. C. Casey, Jr., and K. W. Wecht, J. Appl. Phys. **45**, 2650 (1974).
[39] H. R. Philipp and E. A. Taft, Phys. Rev. **120**, 37 (1960).
[40] M. van Exter and D. J. Grischkovsky, Appl. Phys. Lett. **56**, 1694 (1990).
[41] I. E. Tamm, *Sobranie Nauchnych Trudov* (Nauka, Moscow, 1975), Vol. 1, p. 77; [J. Phys. (USSR) **1**, 439 (1939)].
[42] In general case the total current is distinguished as polarization current associated with bound charges and conduction current related to motion of free charges. This distinction can strictly be made only for static fields and becomes meaningless for time-dependent high-frequency fields. Therefore, the expression for current can be written in two equivalent forms, $\mathbf{J}(\omega) = (\imath\omega)\varepsilon_0\hat{\chi}_{eff}(\omega)\mathbf{E}(\omega)$ and $\mathbf{J}(\omega) = \hat{\sigma}_{eff}(\omega)\mathbf{E}(\omega)$, where $\hat{\chi}_{\mathrm{eff}}(\omega) = \hat{\chi}(\omega) - \frac{\imath\hat{\sigma}(\omega)}{\varepsilon_0\omega}$, $\hat{\sigma}_{eff}(\omega) = \hat{\sigma}(\omega) + \imath\omega\varepsilon_0\hat{\chi}(\omega)$, and $\hat{\sigma}_{eff}(\omega) = (\imath\omega)\varepsilon_0\hat{\chi}_{eff}(\omega)$. High-frequency current $\mathbf{J}(\omega)$ can be treated as transverse polarization charge wave in plasma with $\hat{\chi}_{\mathrm{eff}}(\omega) = \hat{\chi}(\omega) - \frac{\imath\hat{\sigma}(\omega)}{\varepsilon_0\omega}$.
[43] The dispersion of velocities of the pump pulse, v_g, and terahertz EMR, c in the most of materials acquires the form of inequality $c < v_g$ at terahertz frequencies due to contribution of phonons to the dielectric constant and the pump photon energy $\hbar\omega$ well below the band gap E_g (transparency window—$\hbar\omega \ll E_g$). At such condition the source moves faster than EM terahertz wave creating the condition for Vavilov-Cherenkov (VC) effect. Because of VC effect is a noncollinear type of radiation phenomena, it remains beyond the scope of this paper. However, the pump frequencies used in this paper fall in the range $\hbar\omega \sim E_g$. At these frequencies the group dispersion refractive index takes a high value near to $E_g/\hbar$ and at higher frequencies. At these conditions the source, the generation front of photoexcited *e-h* plasma, moves with the velocity satisfying the condition $c \gtrsim v_g$.
[44] B. M. Bolotovskii, Proc. (Tr.) P.N. Lebedev Phys. Inst. **140**, 95 (1982).